A 5-yr Climatology of Severe Convective Wind Events over China

XINLIN YANG

Key Laboratory of Cloud-Precipitation Physics and Severe Storms, Institute of Atmospheric Physics, Chinese Academy of Sciences, and University of Chinese Academy of Sciences, Beijing, China

JIANHUA SUN

Key Laboratory of Cloud-Precipitation Physics and Severe Storms, Institute of Atmospheric Physics, Chinese Academy of Sciences, Beijing, and Collaborative Innovation Center on Forecast and Evaluation of Meteorological Disasters, and Nanjing University of Information Science and Technology, Nanjing, China

YONGGUANG ZHENG

National Meteorological Center, China Meteorological Administration, Beijing, China

(Manuscript received 21 May 2016, in final form 11 April 2017)

ABSTRACT

A method using cloud-to-ground lightning was developed to retrieve severe convective wind (SCW) events from significant weather report data over China during the period 2010–14. The results showed that SCW events were a feature of local weather activity, and their distribution showed clear seasonal and diurnal variations. The SCW events mainly occurred over eastern China during the midafternoon in the warm season and rarely occurred over western China. The highest frequency of SCW events was recorded in north China and Guangdong Province. There was also a high frequency of SCW events in the middle and lower reaches of the Yangtze River. The most frequent occurrence of SCW events was in Guangdong Province in spring, while a high frequency of SCW events was observed in both north China and Guangdong Province during the summer months. The peak month for SCW events was July over the whole of China and June in north China. The pattern in Guangdong Province had a bimodal distribution, with the peak months being May and August. The majority of SCW events occurred between 1200 and 2000 local time.

1. Introduction

Severe convection events generally occur under a favorable synoptic background and are triggered within supportive mesoscale environments. They are often associated with lightning, severe wind, hail, heavy rainfall, and even tornados. Such events can start suddenly at the local scale and often result in disasters. The regulations from the Severe Weather Prediction Center, National Meteorological Center, in China define any wind gust $\geq 17\,\mathrm{m\,s^{-1}}$ as a severe wind event. If a severe wind event was associated with severe thunderstorms, it was classified as a severe convective wind (SCW) in this study; otherwise, it was classified as a nonsevere convective wind (NSCW) event. Severe thunderstorms were defined as those accompanied by more active cloud-to-ground (CG) lightning than the background climatology, detailed in section 2. In China, SCW events result in enormous financial and human costs every year; for example, a shipwreck leading to 442 fatalities was caused by an SCW event in Hubei Province on 1 June 2015. An accurate method of forecasting SCW events is urgently needed to reduce these losses. However, there are many challenges, and it is more difficult for meteorological models and forecasters to predict SCW events than to predict NSCW events. SCW events start suddenly and are generally associated with mesoscale systems lasting for several hours. In contrast, NSCW events such as strong post (cold) frontal winds caused by strong pressure gradients in cold-season synoptic-scale cyclones are longer in duration, can occur over a more widespread area, and are more easily predicted. The goal of this study was to fill gaps in the record of SCW events over China and to perform an analysis of their spatial and temporal

Corresponding author: Dr. Jianhua Sun, sjh@mail.iap.ac.cn

DOI: 10.1175/WAF-D-16-0101.1

distribution. Identifying the climatology of SCW events in China will ultimately lead to improved forecasting of these events.

Both hail and SCW events are severe weather events, but SCW events in China have received less attention than hail events. There have been some studies of the climatology of hail over China (Zhang et al. 2008; Zhang and Gao 2008; Fu et al. 2011), especially for the occurrence of hail in local regions. However, there has been little research on the climatology of SCW events over the whole of China and only a few studies over regional areas, such as Beijing (Qin et al. 2006), eastern China without south China (Yu et al. 2012), and Anhui Province (Zhang et al. 2013). Because there are no special data or records to clarify SCW events in China, previous studies have based their results on stations with wind speeds exceeding a defined threshold on a day on which a thunderstorm occurred at that station. However, some of these events may have been contaminated by NSCW events. For example, wind speeds are often high at observation stations located on mountains or islands. Sometimes even a weak thunderstorm may be sufficient to push wind speeds over the $17\,m\,s^{-1}$ threshold for a severe wind event, thus, seeming to qualify such a wind gust as an SCW event. However, this kind of event should not be considered an SCW event because SCW events are generally caused by a strong downdraft from deep moist convection. Therefore, these kinds of severe wind events were affected by orographic action. Consequently, the accurate selection of SCW events is a key process in determining the climatology of SCW events in China.

The United States also suffers considerable losses from SCW events. SCW events cause an average of 84 fatalities in the United States each year (Ashley 2007; Black and Ashley 2010). These events have been studied in the United States for a long time, and there the amount of data available regarding the climatology of SCW events is vast. Kelly et al. (1985) showed that 61% of thunderstorm-related SCW events in the United States typically occur during the midafternoon in June and July. Klimowski et al. (2003) reported that SCW events showed clear seasonal and diurnal variations over the northern plains of the United States. SCW events predominantly occur over the eastern Rocky Mountains and significant SCW ($\geq 33.4\,m\,s^{-1}$) events mainly occur over the Great Plains (Doswell et al. 2005). There is a distinct spatial pattern to SCW events, with the high plains receiving the greatest number of events and a secondary corridor extending from the central plains to the Midwest and the Ohio valley (Smith et al. 2013). There have also been many published reports of the climatology of derechos [convection-induced wind storms; Johns and Hirt (1987); Bentley and Mote (1998); Bentley and Sparks (2003); Coniglio and Stensrud (2004); Ashley and Mote (2005)]. Derechos often produce SCW events; for example, in a derecho over Guangdong Province in China, gales persisted for 6 h, with a major axis length of 350 km (Xia et al. 2012).

The rest of this paper is organized as follows. The data and methods are discussed in section 2. Then results are presented and discussed in section 3. Finally, a summary and our conclusions are given in section 4.

2. Data and methods

The SCW events were derived from significant weather report (SWR) data from the China Meteorological Administration for the period 2010–14. There are eight 3-h files for each day in the SWR dataset. The SWR data contain information on significant weather events, such as thunderstorms, wind events, hail, and dust storms. The SWR data include the station ID, location, time, and type of weather phenomena. However, the weather type was not specified for some severe wind entries. There were 2403 stations in the SWR dataset during 2010–14 (Fig. 1): 2063 stations (about 86%) had 5 yr of reports, 108 had 4 yr, 99 had 3 yr, 104 had 2 yr, and 29 had 1 yr. SWR data were not recorded during a portion of the study period at these stations, among them were 183 stations in Xinjiang and Guizhou Provinces. Stations with only 1 or 2 yr of records were mainly located in these two regions (Figs. 1 and 2b). The main reason for this was that 110 stations in 2012 and 183 in 2013–14 were missing SWR data in these provinces.

The 2403 stations were interpolated onto a $2^\circ \times 2^\circ$ map and binned by location to illustrate the spatial distribution of the observing stations (Fig. 2a). The greatest station densities were over the eastern Taihang Mountains, such as Hebei, northern Henan, and western Shandong Provinces, where there were more than 35 stations per grid box (Figs. 2a,b). In addition, a region in the middle and lower reaches of the Yangtze River valley, south China, and the Sichuan basin had more than 25 stations per grid box. For most other areas, the station density was less than 20 stations per grid box. The number of reports was affected by the uneven population density, which was similar to the situation in the United States (Weiss et al. 2002). This uneven distribution of stations will affect the spatial and temporal distribution of SCW events. To minimize the impact of this, the SCW data were normalized by dividing the total number of SCW events by the number of stations at each grid point.

Radar, satellite, and CG lightning data have the potential to distinguish between SCW and NSCW events, but satellite data have a coarser temporal resolution than CG or radar data. Radar data are not available over

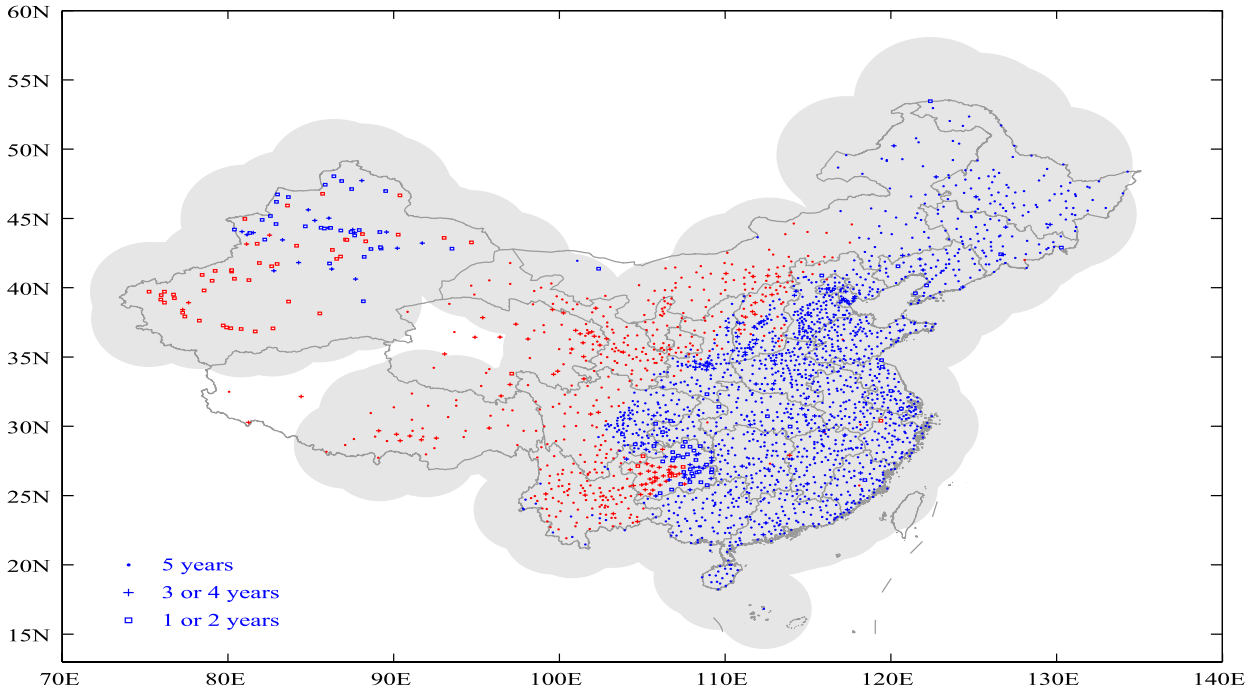

FIG. 1. Distribution of stations recording SWR data during 2010–14. Dots represent the stations that have a 5-yr record, crosses represent stations with 3- or 4-yr records, and squares represent stations with 1- or 2-yr records. Red (blue) symbols mean that the station altitude is greater (less) than 1000 m. The gray shading is the region where lightning flashes can be detected within 300 km of a sensor.

western China and do not record data throughout the day during nonflood seasons. CG lightning can be detected over almost all of China, except for parts of the Tibetan Plateau (the unshaded area in Figs. 1 and 2b). After comparing the detection range and spatiotemporal resolution of the radar, satellite, and CG lightning data, CG lightning data were selected to distinguish between SCW and NSCW events.

The China Lightning Detection Network (CLDN) consists of 357 sensors across most of China. The detection efficiency of CLDN claimed by the instructions from the manufacturer is between 80% and 90%, and the actual detection efficiency could be much lower in some regions, for example over the Tibetan Plateau and western China, because of the lower concentration of sensors and complex terrain. The CLDN uses the Improved Performance through Combined Technology (IMPACT) method, which combines directional information and time-of-arrival technology to determine the location of lightning, and is similar to the method used in the U.S. National

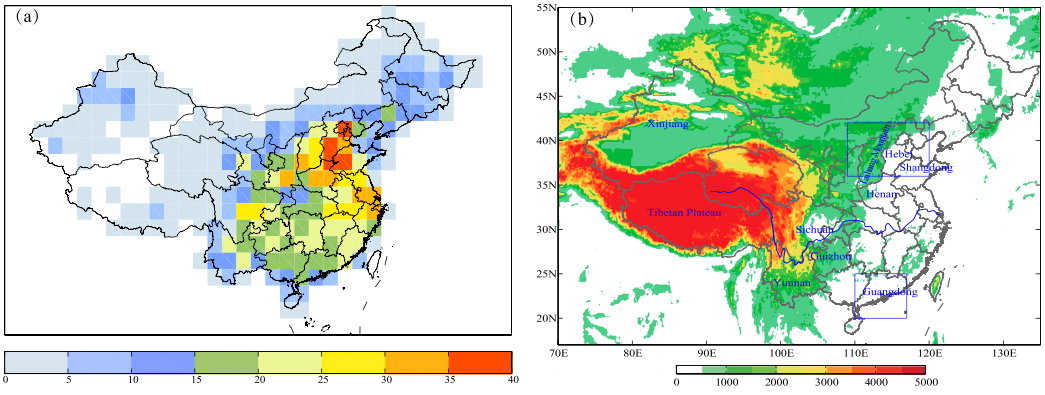

FIG. 2. (a) Spatial distribution of station density with a resolution of 2° × 2°. (b) Distribution of terrain in China (m). The blue line represents the Yangtze River. The lower blue rectangle (20°–25°N, 110°–117°E) covers most of Guangdong Province. The upper blue rectangle (36°–42°N, 109°–120°E) represents the region of north China.

Lightning Detection Network (Cummins et al. 1998). Positive CG flashes with a peak current < 10 kA were deleted (Liu et al. 2011, 2013; Zheng et al. 2009, 2016) because they could have been contaminated by cloud-to-cloud lightning (Cummins et al. 2006) and have an extremely low detection efficiency (Cummins and Murphy 2009; Enno 2011).

A strong connection between CG lightning and convective activity has been indicated by previous studies (Goodman et al. 1988; Reap and MacGorman 1989; Carey and Buffalo 2007; Feng et al. 2007, 2009), and CG lightning has been used to track thunderstorm cells (Betz et al. 2008; Kohn et al. 2011). SCW events occurred at almost the central point of areas of high CG density (Yang and Sun 2014). The convective activity associated with SCWs is in general more intense than convective activity occurring without an SCW event. Therefore, if a severe wind event was associated with a higher density of CG lightning than the climatic background state, it was classified as an SCW event.

The main data processing was conducted as follows. First, the events with wind speeds $\geq 17\,\mathrm{m\,s^{-1}}$ during 2010–14 were selected from the SWR dataset. According to the China Meteorological Administration, a new report is required if the magnitude of the wind speed is reinforced or a mistake is found in a previous report. Therefore, there may be multiple reports within the SWR dataset for the same wind event. Where this was the case, the later report was saved and the other reports were removed. To avoid the influence of typhoons, reports were discarded when the distance between the location of the wind and the center of the typhoon was <800 km. Typhoon best-track data were obtained from the National Meteorological Center in China.

The number of CG lightning flashes in four different-sized boxes (0.5° latitude × 0.5° longitude, 1° × 1°, 1.5° × 1.5°, and 2° × 2°) around the location of the candidate severe wind report from half an hour before the event to half an hour after the event were calculated. The numbers of CG lightning flashes in the four boxes were expressed by N_1, N_2, N_3, and N_4, respectively. Because mesoscale convective systems range from tens to hundreds of kilometers in scale, the four regions represented the variation in the horizontal scale for these convective systems. CG lightning activity displayed an obvious monthly variation over China (Yang et al. 2015), and the frequency of CG lightning events over China also varied (Qie et al. 2005, 2009; Zheng et al. 2009; Liu et al. 2011, 2013). Therefore, the CG intensity of an event was compared with the climatic background intensity in the same month in which the severe wind report occurred. The background number of CG lightning flashes N over a 2° × 2° region, the center of which lay at the location of each potential SCW event, was then calculated during the corresponding month for each of the five years. Let T be the number of hours in which climatic background lightning flashes occurred, making the climatic background flash rate N/T. The intensity of the CG lightning flashes per unit area and per unit time was compared between the four regions and with the 5-yr climatological value. A candidate wind report was classified as an SCW event if 1) $N_4 \geq 10$ to ensure that each SCW event was associated with intense convection and 2) one of the following inequalities was true: $N_1/t > (1/16)N/T$; $N_2/t > (1/4)N/T$; $N_3/t > (9/16)N/T$; and $N_4/t > N/T$, where t was 1 h.

3. Characteristics of SCW events

There were 1171 stations with 5497 severe wind events in the 5-yr SWR dataset. A total of 1019 stations with 3121 SCW events were classified (Fig. 3a). The highest number of events (821) occurred in 2011, accounting for 26% of the total, whereas the lowest number of events (382) occurred in 2012, accounting for 12% of the total. The number of events in the other three years varied between 520 and 707. The highest number of stations with SCW events also occurred in 2011: 498 (49%) stations (Fig. 3b). The lowest number of stations was 291 (29%) in 2012. The number of stations with SCW events in the other three years varied between 365 and 458. This showed that there was considerable annual variation in the frequency and location of the SCW events.

a. Spatial distribution of SCW events

The annual average number of SCW events was <1 for 80% of the stations and 39% of stations had just a single SCW event during the study period (Fig. 4). Only 45 stations (4%) had two or more SCW events per year, and these stations were mainly located in north China and Guangdong Province. In general, SCW events occurred less than once per year for most stations.

Figure 5a shows the spatial distribution of normalized SCW events from 2010 to 2014. The highest frequency of SCW events was recorded in north China and Guangdong Province. There was also a high frequency of SCW events in the middle and lower reaches of the Yangtze River. SCW events rarely occurred in western China. The three regions with a high frequency of SCW events were rainfall belts during the warm season over eastern China (Tao 1980). Therefore, a strong relation was found between the regions with a high frequency of SCW events and the rainfall belts.

Because north China and Guangdong Province had a high frequency of both severe wind and SCW events (Figs. 5a,b), this study focused on the characteristics of SCW events over north China and Guangdong Province.

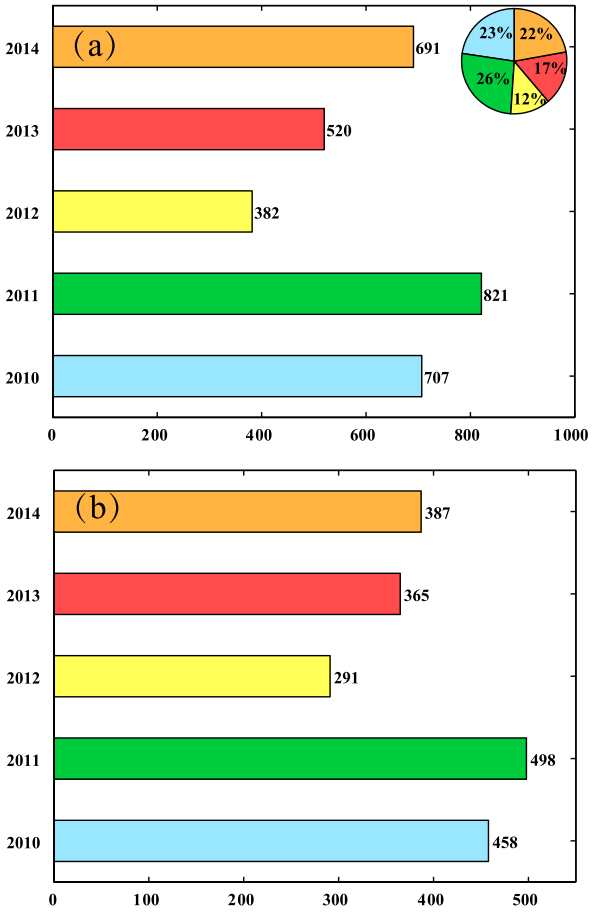

FIG. 3. (a) Annual frequency (bar chart) of SCW events in 2010–14 and the corresponding percentages (pie chart). (b) Annual frequency of the stations recording SCW events during 2010–14.

The proportion of SCW events to severe wind events (Fig. 5c) was >70% in southern China, which was significantly larger than in northern China. The proportion of SCW events to severe wind events was <60% over mountainous areas in north China. This means that about 40% of severe wind events were NSCW events in the mountainous regions of north China, which may be a consequence of the combined action of the strong pressure gradients accompanying strong synoptic-scale cyclones and the presence of high mountains. Of the four paths along which strong, cold air invades China, three pass through north China (Zhu et al. 1981). Therefore, stations over mountainous areas in north China experienced more NSCW events than other regions in eastern China.

b. Seasonal variation of SCW events

There was a clear seasonal variation in SCW events in China. From the monthly variation in the frequency of SCW events (Fig. 6a), it can be seen that the warm season was the period when most SCW events occurred, while they were essentially absent during January and December. Some studies of regional SCW events have shown similar results (Qin et al. 2006; Zhang et al. 2013; Yan et al. 2013). The peak month for SCW events over the whole of China was July (Fig. 6a). In China, 91.3% of SCW events occurred in spring (March–May) and summer (June–August) and 69.4% occurred in summer (Fig. 6b). SCW events in winter (December–February) accounted for only 0.7% of the total, and all of them occurred in February (Figs. 6a,b). The peak month for SCW events was June in north China, whereas the pattern in Guangdong Province had a bimodal distribution, with the two peak months being May and August (Fig. 6a). About 94% of SCW events over Guangdong Province occurred between March and August, whereas most SCW events (95.3%) occurred between May and September over north China. Over Guangdong Province, the proportion of SCW events in summer was 52.4%, slightly larger than in spring (41.7%) (Fig. 6d). No SCW event occurred in these two regions during the three winter months (Figs. 6c,d).

The spatial distribution of SCW events also displayed a clear seasonal variation in China. The spatial distribution in summer was similar to the 5-yr distribution, with two high-frequency regions (not shown). The SCW events over the middle and lower reaches of the Yangtze River valley mostly occurred in summer. In spring, the highest frequency of SCW events was in Guangdong Province, while the frequency in other parts of eastern China was smaller (not shown). The second highest frequency of events was in north China, but it was much less than that in Guangdong Province. The number of SCW events gradually decreased from autumn (September–November) to winter over China. SCW events in winter mainly occurred over the middle and lower reaches of the Yangtze River valley.

Figure 7 shows the spatial distribution of the proportion of total yearly SCW events occurring in spring and summer. The SCW events in north China mainly occurred in summer, and a similar proportion of SCW events occurred in spring and summer in Guangdong Province. More than 60% of SCW events over China occurred during summer, except in Yunnan Province, south China, and some grid points across northern China (Fig. 7b). In Yunnan Province, the majority of SCW events occurred in spring (Fig. 7a), which is consistent with previous studies (Tao et al. 2002; Tao et al. 2011). Tao et al. (2002) indicated that hail events mainly occurred during February–April in Yunnan. The proportion of SCW events at some scattered grid points over northern China reached 90% in spring (Fig. 7a) because there were only one or two SCW events in these grids during the 5 yr of reports, and all of them occurred

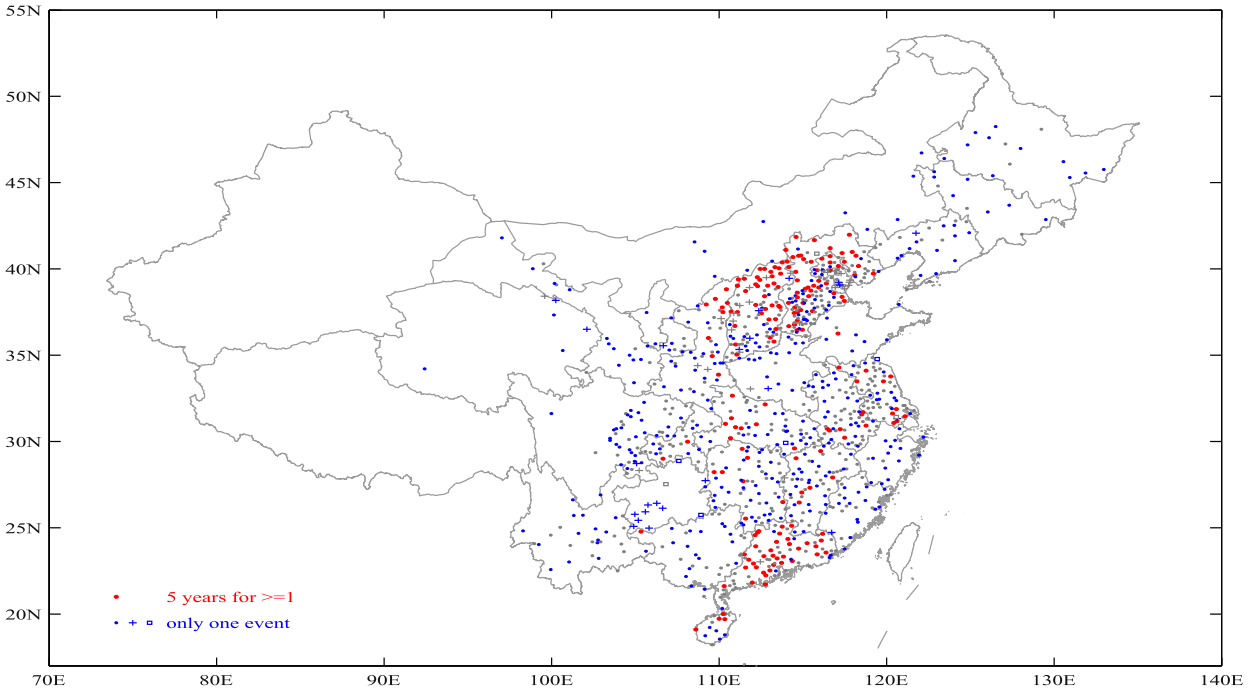

FIG. 4. Distribution of SCW events. Dots represent the stations that have a 5-yr record, crosses represent stations with 3- or 4-yr records, and squares represent stations with 1- or 2-yr records. Red dots represent the stations that have an annual average of SCW events equal to or greater than one. Blue markers are the stations with only one SCW event.

in spring. More data from additional observation periods are needed to better estimate the seasonal distribution of SCW events in northern China.

The monthly variation in the number of SCW events by latitude (Fig. 8) suggests that SCW events occurred in three major zones: north China (36°–42°N), Guangdong Province (20°–25°N), and the middle and lower reaches of the Yangtze River valley (28°–33°N). The latitude associated with SCW events gradually expanded northward from February to June. There was a seasonally constant local maximum in SCW events in the 20°–25°N band (from March to August), which contained the latitudinal maximum across all of China during the early portion from March to May. The number of SCW events increased in May in the 35°–40°N band, where there was a high frequency in June and July. SCW events were prevalent in China during July and August and clearly increased from 28° to 33°N. The highest frequency of SCW events shifted to the 28°–33°N band in August.

c. *Diurnal variation of SCW events*

Figure 9 shows the diurnal distribution of SCW events over China, Guangdong Province, and north China. SCW events most commonly occurred during the mid-afternoon (1200–2000 local time) in these three regions, with 84.1%, 78.7%, and 87.8% of all events occurring at these times, respectively (Fig. 9a). The common pattern was an increase in the number of events beginning at

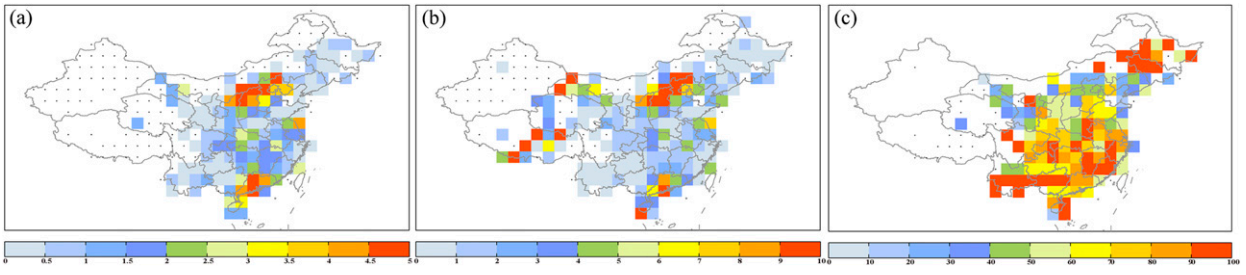

FIG. 5. (a) Spatial distribution of SCW events after normalization (events per station per unit time) during 2010–14. Dots represent a grid with stations, but without SCW events. (b) As in (a), but for severe wind events during 2010–14. (c) Spatial distribution of the proportion of SCW events to severe wind events (%). Dots represent grids with severe winds, but without SCW events.

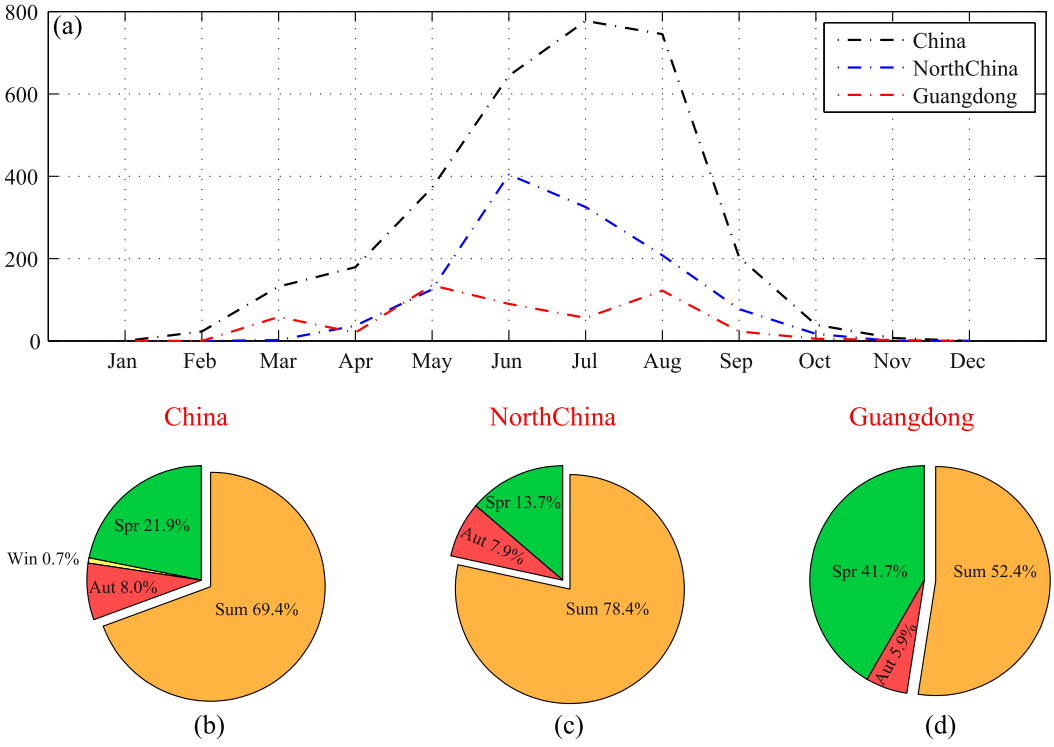

FIG. 6. (a) Monthly distribution of SCW events over China, north China (36°–42°N, 109°–120°E), and Guangdong Province (20°–25°N, 110°–117°E). Proportion of each season's events during a full year for (b) China, (c) north China, and (d) Guangdong.

1200 local time and a decrease at 1900 local time. Some previous studies of regional SCW events have shown similar results (Liang et al. 2006; Qin et al. 2006; Zhang et al. 2013; Yan et al. 2013). However, there were some significant differences in the diurnal variation over the three regions. The peak period was from 1500 to 1800 local time (LT) over China as a whole, 1400 to 1700 LT in Guangdong Province, and 1600 to 1800 LT in north China (Fig. 9b). A comparison of the proportions of SCW events between 0600 and 1200 local morning time over the two regions with the most SCW events showed that the value for Guangdong (17%) was greater than that for north China (1.5%). Zhang and Gao (2008) obtained a similar result for hail events between north China and south China. This may be because the trigger for the initiation of convection differed between regions. The western region of north China consists of high mountains, whereas the eastern part consists of plains.

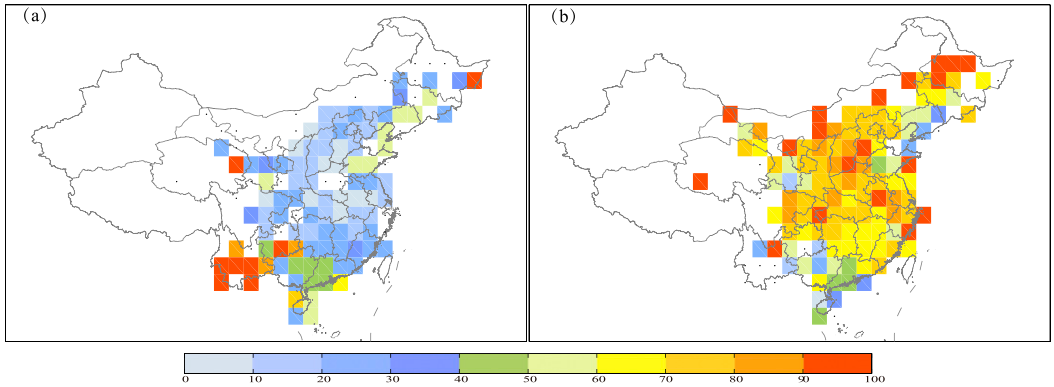

FIG. 7. Spatial distribution of the proportion of total yearly SCW events occurring during (a) spring and (b) summer. Dots represent grids with severe winds, but without SCW events (%).

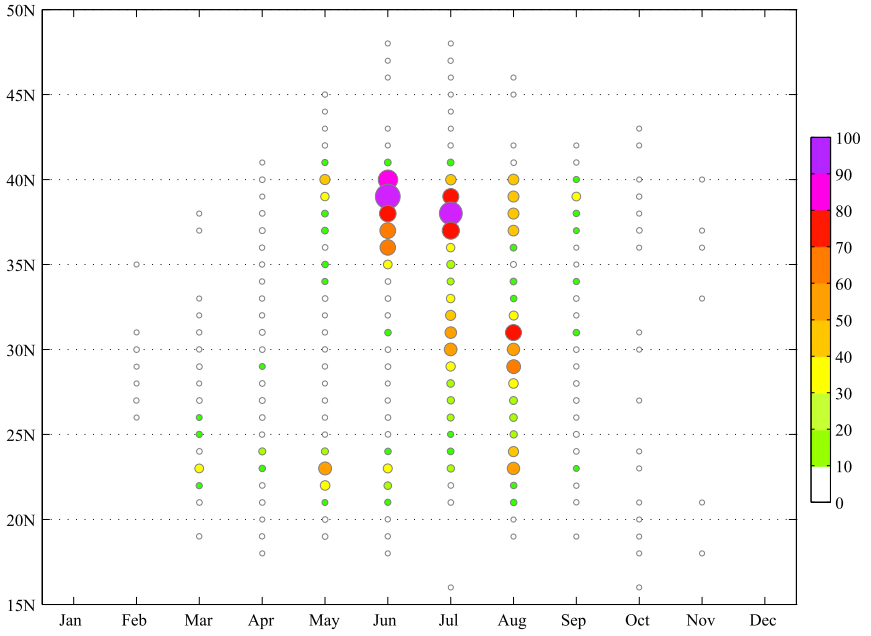

FIG. 8. Monthly variation in the number of SCW events at different latitudes (time). The dots are also sized and colored according to the total count.

The southern part of Guangdong Province is flatter than the northern part of Guangdong Province, which is hilly. The elevation gradient over north China is clearly larger than over Guangdong Province (Fig. 2b). A local circulation that can trigger convection during the early afternoon forms more easily near mountain ranges (He and Zhang 2010), and therefore SCW events occurred more frequently during the afternoon over north China than over south China.

4. Discussion and conclusions

To select SCW events and understand their climatology, a method was developed to distinguish between SCW and NSCW events using CG lightning data. CG lightning and SWR data were used to identify SCW events over China from 2010 to 2014, and their spatial and temporal distributions were analyzed.

SCW events mainly occurred in eastern China, but only rarely occurred over northwest China and the Tibetan Plateau. The high-frequency regions for SCW events were north China and Guangdong Province, with a secondary area in the middle and lower reaches of the Yangtze River valley. SCW events displayed significant seasonal and diurnal variations. SCW events in China were prevalent during the midafternoon in spring and summer, with 91.3% of SCW events occurring during these two seasons, and about 69% of events occurring during summer. In spring the highest frequency of SCW events occurred in Guangdong Province. The frequency of SCW events in north China increased further during summer. SCW events over the middle and lower Yangtze River valley mainly occurred in summer. About 78% of SCW events occurred in summer in north China, whereas the proportion of SCW events occurring over Guangdong Province was 52.4% during the summer, slightly larger than the value of 41.7% in spring. The majority of SCW events over China took place between 1200 and 2000 local time. There was a common tendency for the number of SCW events to increase after 1200 local time and to decrease at 1900 local time.

The SCW events over China only occurred from February to November, with a peak in July. The peak month for north China was June, whereas the pattern for Guangdong Province showed a bimodal distribution with two peaks in May and August. The northernmost latitude with SCW events expanded northward from February to June. However, the latitudinal zones with the most active SCW events varied among the different months. The SCW events over these latitudinal zones mainly occurred in Guangdong Province, the middle and lower reaches of the Yangtze River, and north China.

The spatial and temporal characteristics are affected by the distribution of stations, especially in regions without stations. The results for the Xinjiang and Guizhou Provinces should be interpreted with caution because two years' worth of records are missing. If SCW events occur with few CG lightning flashes, the method may not record

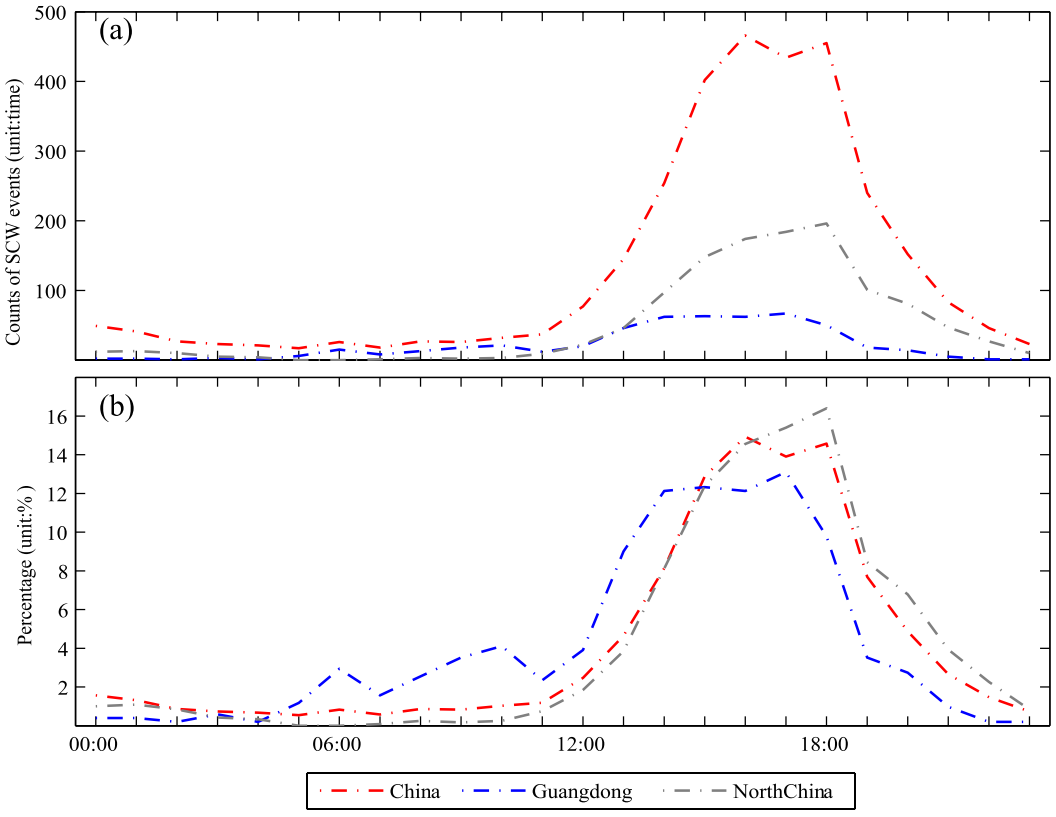

FIG. 9. (a) Diurnal variation of SCW events over China, Guangdong Province (20°–25°N, 110°–117°E), and north China (36°–42°N, 109°–120°E). (b) Proportion of SCW events (%) during each hour of the day for these three regions.

an SCW event during the cold season. However, most convection in China takes place during the warm season when CG lightning activity is vigorous. Severe winds can occur over the Tibetan Plateau, where SCW cases are rare. Thunderstorms are generally weak over the Tibetan Plateau (Zhang et al. 1998; Qie et al. 2002). Because CG lightning was used to classify SCW events, the results may have been influenced by the efficiency of the CLDN sensors. Severe wind events were not only affected by the atmospheric conditions, but also by the topography. SCW events do not often occur west of the Rocky Mountains in North America (Doswell et al. 2005; Smith et al. 2013). These severe winds are categorized as NSCW events, a classification that may have been influenced by the high altitude of the recording stations or other weather systems. Some stations often appeared to experience severe winds, but few of these events were classified as SCW events because the stations were located on high mountains or offshore islands.

SCW events mainly occurred during the midafternoon in the warm season. Favorable conditions prevailed, where the lower-tropospheric air became much warmer in the midafternoon because of the absorption of solar radiation. Once the warm air was lifted, the convective available potential energy was released, allowing SCW events to occur. Toumi and Qie (2004) indicated that the heat flux played an important part in the generation of convection. It is important to know the threshold value of the convective available potential energy when SCW events occur. Sometimes the atmosphere meets the threshold value of convective available potential energy, while SCW events may not occur without the forcing of convection initiation. It is clear that the trigger mechanism for an SCW event varies in different regions and in different seasons. Future studies are needed to determine the trigger mechanisms for SCW events in north China and Guangdong Province.

Acknowledgments. The CG lightning and SWR data were provided by the National Meteorological Center and the Meteorological Observation Center in China. This research was supported by the China Meteorological Administration (Grant GYHY201406002), the Key Program of the Chinese Academy of Sciences (Grant 2013CB430101), and the National Natural Science Foundation of China (Grant 41375051).

REFERENCES

Ashley, W. S., 2007: Spatial and temporal analysis of tornado fatalities in the United States: 1880–2005. *Wea. Forecasting*, **22**, 1214–1228, doi:10.1175/2007WAF2007004.1.

——, and T. L. Mote, 2005: Derecho hazards in the United States. *Bull. Amer. Meteor. Soc.*, **86**, 1577–1592, doi:10.1175/BAMS-86-11-1577.

Bentley, M. L., and T. L. Mote, 1998: A climatology of derecho-producing mesoscale convective systems in the central and eastern United States, 1986–95. Part I: Temporal and spatial distribution. *Bull. Amer. Meteor. Soc.*, **79**, 2527–2540, doi:10.1175/1520-0477(1998)079<2527:ACODPM>2.0.CO;2.

——, and J. A. Sparks, 2003: A 15-year climatology of derecho producing mesoscale convective systems over the central and eastern United States. *Climate Res.*, **24**, 129–139, doi:10.3354/cr024129.

Betz, H. D., K. Schmidt, W. P. Oettinger, and B. Montag, 2008: Cell-tracking with lightning data from LINET. *Adv. Geosci.*, **17**, 55–61, doi:10.5194/adgeo-17-55-2008.

Black, A. W., and W. S. Ashley, 2010: Nontornadic convective wind fatalities in the United States. *Nat. Hazards*, **54**, 355–366, doi:10.1007/s11069-009-9472-2.

Carey, L. D., and K. M. Buffalo, 2007: Environmental control of cloud-to-ground lightning polarity in severe storms. *Mon. Wea. Rev.*, **135**, 1327–1353, doi:10.1175/MWR3361.1.

Coniglio, M. C., and D. J. Stensrud, 2004: Interpreting the climatology of derechos. *Wea. Forecasting*, **19**, 595–605, doi:10.1175/1520-0434(2004)019<0595:ITCOD>2.0.CO;2.

Cummins, K. L., and M. J. Murphy, 2009: An overview of lightning locating systems: History, techniques, and data uses, with an in-depth look at the US NLDN. *IEEE Trans. Electromagn. Compat.*, **51**, 499–518, doi:10.1109/TEMC.2009.2023450.

——, ——, E. A. Bardo, W. L. Hiscox, R. B. Pyle, and A. E. Pifer, 1998: A combined TOA/MDF technology upgrade of the U.S. National Lightning Detection Network. *J. Geophys. Res.*, **103**, 9035–9044, doi:10.1029/98JD00153.

——, J. A. Cramer, C. J. Biagi, E. P. Krider, J. Jerauld, M. A. Uman, and V. A. Rakov, 2006: The U.S. National Lightning Detection Network: Post-upgrade status. *Second Conf. on Meteorological Applications of Lightning Data*, Atlanta, GA, Amer. Meteor. Soc., 6.1. [Available online at http://ams.confex.com/ams/pdfpapers/105142.pdf.]

Doswell, C. A., III, H. E. Brooks, and M. P. Kay, 2005: Climatological estimates of daily local nontornadic severe thunderstorm probability for the United States. *Wea. Forecasting*, **20**, 577–595, doi:10.1175/WAF866.1.

Enno, S. E., 2011: A climatology of cloud-to-ground lightning over Estonia, 2005–2009. *Atmos. Res.*, **100**, 310–317, doi:10.1016/j.atmosres.2010.08.024.

Feng, G., X. Qie, T. Yuan, and S. Niu, 2007: Analysis on lightning activity and precipitation structure of hailstorms. *Sci. Chin. Ser. Dokl. Earth Sci.*, **50**, 629–639.

——, ——, J. Wang, and D. Gong, 2009: Lightning and Doppler radar observations of a squall line system. *Atmos. Res.*, **91**, 466–478, doi:10.1016/j.atmosres.2008.05.015.

Fu, L., W. Li, P. Zhang, Q. Zhang, and G. Gao, 2011: Inter-decadal change of hail events over China and causation analysis in northern China in recent 50 years (in Chinese). *Meteor. Mon.*, **37**, 669–676.

Goodman, S. J., D. E. Buechler, P. D. Wright, and W. D. Rust, 1988: Lightning and precipitation history of a microburst-producing storm. *Geophys. Res. Lett.*, **15**, 1185–1188, doi:10.1029/GL015i011p01185.

He, H., and F. Zhang, 2010: Diurnal variations of warm-season precipitation over northern China. *Mon. Wea. Rev.*, **138**, 1017–1025, doi:10.1175/2010MWR3356.1.

Johns, R. H., and W. D. Hirt, 1987: Derechos: Widespread convectively induced windstorms. *Wea. Forecasting*, **2**, 32–49, doi:10.1175/1520-0434(1987)002<0032:DWCIW>2.0.CO;2.

Kelly, D. L., J. T. Schaefer, and C. A. Doswell III, 1985: Climatology of nontornadic severe thunderstorm events in the United States. *Mon. Wea. Rev.*, **113**, 1997–2014, doi:10.1175/1520-0493(1985)113<1997:CONSTE>2.0.CO;2.

Klimowski, B. A., M. J. Bunkers, M. R. Hjelmfelt, and J. N. Covert, 2003: Severe convective windstorms over the northern high plains of the United States. *Wea. Forecasting*, **18**, 502–519, doi:10.1175/1520-0434(2003)18<502:SCWOTN>2.0.CO;2.

Kohn, M., E. Galanti, C. Price, K. Lagouvardos, and V. Kotroni, 2011: Nowcasting thunderstorms in the Mediterranean region using lightning data. *Atmos. Res.*, **100**, 489–502, doi:10.1016/j.atmosres.2010.08.010.

Liang, A., Q. Zhang, H. Shen, X. Li, and K. Wang, 2006: Application of NCEP data and Doppler weather radar data to thunderstorm prediction in Beijing area (in Chinese). *Meteor. Mon.*, **32**, 73–80.

Liu, D., X. Qie, Y. Xiong, and G. Feng, 2011: Evolution of the total lightning activity in a leading-line and trailing stratiform mesoscale convective system over Beijing. *Adv. Atmos. Sci.*, **28**, 866–878, doi:10.1007/s00376-010-0001-8.

——, ——, L. Pan, and L. Peng, 2013: Some characteristics of lightning activity and radiation source distribution in a squall line over north China. *Atmos. Res.*, **132–133**, 423–433, doi:10.1016/j.atmosres.2013.06.010.

Qie, X., Y. Yu, D. Wang, H. Wang, and R. Chu, 2002: Characteristics of cloud-to-ground lightning in Chinese inland plateau. *J. Meteor. Soc. Japan*, **80**, 745–754, doi:10.2151/jmsj.80.745.

——, T. Zhang, C. Chen, G. Zhang, T. Zhang, and W. Wei, 2005: The lower positive charge center and its effect on lightning discharges on the Tibetan Plateau. *Geophys. Res. Lett.*, **32**, L05814, doi:10.1029/2004GL022162.

——, ——, G. Zhang, and T. Zhang, 2009: Electrical characteristics of thunderstorms in different plateau regions of China. *Atmos. Res.*, **91**, 244–249, doi:10.1016/j.atmosres.2008.04.014.

Qin, L., D. Li, and S. Gao, 2006: The synoptic and climatic characteristics studies of thunderstorms winds in Beijing (in Chinese). *Climatic Environ. Res.*, **11**, 754–766.

Reap, R. M., and D. R. MacGorman, 1989: Cloud-to-ground lightning: Climatological characteristics and relationships to model fields, radar observations, and severe local storms. *Mon. Wea. Rev.*, **117**, 518–535, doi:10.1175/1520-0493(1989)117<0518:CTGLCC>2.0.CO;2.

Smith, B. T., T. E. Castellanos, A. C. Winters, C. M. Mead, A. R. Dean, and R. L. Thompson, 2013: Measured severe convective wind climatology and associated convective modes of thunderstorms in the contiguous United States, 2003–09. *Wea. Forecasting*, **28**, 229–236, doi:10.1175/WAF-D-12-00096.1.

Tao, S. Y., 1980: *Rainstorms in China* (in Chinese). Science Press, 225 pp.

Tao, Y., X. Duan, and M. Yang, 2002: Study on spatial-temporal distribution and climate causes of hail formation in Yunnan (in Chinese). *J. Nanjing Inst. Meteor.*, **25**, 837–842.

——, ——, C. Duan, and W. Duan, 2011: Change characteristic of Yunnan hail (in Chinese). *Plateau Meteor.*, **30**, 1108–1118.

Toumi, R., and X. Qie, 2004: Seasonal variation of lightning on the Tibetan Plateau: A spring anomaly? *Geophys. Res. Lett.*, **31**, L04115, doi:10.1029/2003GL018930.

Weiss, S. J., J. A. Hart, and P. R. Janish, 2002: An examination of severe thunderstorm wind report climatology: 1970–1999. *21st Conf. on Severe Local Storms*, San Antonio, TX, Amer. Meteor. Soc., 11B.2. [Available online at https://ams.confex.com/ams/pdfpapers/47494.pdf.]

Xia, R., D. Wang, J. Sun, G. Wang, and G. Xia, 2012: An observational analysis of a derecho in South China. *Acta Meteor. Sin.*, **26**, 773–787, doi:10.1007/s13351-012-0608-z.

Yan, S., Y. Li, L. Qi, J. An, and J. Liu, 2013: Analysis and application of thermo-dynamical and dynamical indexes associated with thunderstorm gale in North China (in Chinese). *Torrential Rain Disaster*, **32**, 17–23.

Yang, X.-L., and J. Sun, 2014: The characteristics of cloud-to-ground lightning activity with severe thunderstorm wind in South and North China. *Atmos. Ocean. Sci. Lett.*, **7**, 571–576, doi:10.3878/AOSL20140046.

——, ——, and W. Li, 2015: An analysis of cloud-to-ground lightning in China during 2010–13. *Wea. Forecasting*, **30**, 1537–1550, doi:10.1175/WAF-D-14-00132.1.

Yu, R., X. Zhang, G. Li, and Q. Gao, 2012: Analysis of frequency of variation of thunderstorm, hail and gale wind in eastern China from 1971 to 2000 (in Chinese). *Meteor. Mon.*, **38**, 1207–1216.

Zhang, C., Q. Zhang, and Y. Wang, 2008: Climatology of hail in China: 1961–2005. *J. Appl. Meteor. Climatol.*, **47**, 795–804, doi:10.1175/2007JAMC1603.1.

Zhang, F., and H. Gao, 2008: Temporal and spatial features of hail days in China (in Chinese). *J. Nanjing Inst. Meteor.*, **31**, 687–693.

Zhang, X., Z. Zhu, and G. Liu, 2013: Spatial-temporal variation characteristics of thunderstorm wind of Anhui province in recent 40 years (in Chinese). *Resour. Environ. Yangtze Basin*, **22**, 1621–1626.

Zhang, Y. J., Z. M. Ge, Z. P. Cheng, and Q. Meng, 1998: Electrical characteristics of atmosphere in east area of Qinghai-Xizang plateau (in Chinese). *Plateau Meteor.*, **17**, 135–140.

Zheng, D., Y. Zhang, Q. Meng, W. Lu, and X. Yi, 2009: Total lightning characteristics and electric structure evolution in a hailstorm. *Acta Meteor. Sin.*, **23**, 233–249.

——, ——, ——, L. W. Chen, and J. R. Dan, 2016: Climatology of lightning activity in South China and its relationship to precipitation and convective available potential energy. *Adv. Atmos. Sci.*, **33**, 365–376, doi:10.1007/s00376-015-5124-5.

Zhu, Q. G., J. R. Lin, and S. W. Shou, 1981: *Principles and Methods in Synoptic Meteorology* (in Chinese). China Meteorological Press, 535 pp.